경사기능재료 판의 최적설계
Optimal Design of Functionally Graded Plates

나경수† ·김지환*
Kyung-Su Na and Ji-Hwan Kim

Key Words : Functionally Graded Materials (경사기능재료), Stress Analysis (응력해석), Thermo-Mechanical Buckling (열-기계적 좌굴), Optimal Design (최적설계)

ABSTRACT

Optimal design of functionally graded plates is investigated considering stress and critical temperature. Material properties are assumed to be temperature dependent and varied continuously in the thickness direction. The effective material properties are obtained by applying linear rule of mixtures. The 3-D finite element model is adopted using an 18-node solid element to analyze more accurately the variation of material properties and temperature field in the thickness direction. For stress analysis, the tensile stress ratio and compressive stress ratio of the structure under mechanical load are investigated. In the thermo-mechanical buckling analysis, temperature at each node is obtained by solving the steady-state heat transfer problem and Newton-Raphson method is used for material nonlinear analysis. Finally, the optimal design of FGM plates is studied for stress reduction and improving thermo-mechanical buckling behavior, simultaneously.

1. Introduction

Functionally graded materials (FGMs) are spatial composites in which material properties vary continuously from one surface to the other. Typically FGMs are made from a ceramic and metal. By mixing these materials, a FGM can withstand high-temperature environments while maintain their structural integrity. Due to these advantages, FGMs have been introduced and applied to many engineering parts (1).

Na and Kim (2) analyzed nonlinear bending of functionally graded plates subjected to uniform pressure and thermal loads using 3-D finite element method. A three-dimensional solid element was used. The Green-Lagrange nonlinear strain-displacement relation and the incremental formulation were adopted for nonlinear analysis. The thermal loads were assumed as uniform, linear and sinusoidal temperature rises across the thickness direction. Na and Kim (3) also investigated the three-dimensional thermo-mechanical buckling of fully FGM plates or FGM composite plates by using finite element method. In these, 18-node solid elements and the assumed strain mixed formulation were applied. The thermal buckling behavior under time-dependent or time-independent temperature rise was analyzed. Oota et al. (4) applied a genetic algorithm to an optimization problem of minimizing the thermal stress distribution for a plate of step-formed FGMs. The step-formed FGM plate was analyzed as a laminated composite plate made of numerous layers with homogeneous and different isotropic material properties.

In this work, stress analysis under mechanical load, thermo-mechanical buckling behavior and optimal design of FGM plates are investigated. Material properties are assumed to be temperature dependent and varied continuously in the thickness direction. The effective material properties are obtained by applying linear rule of mixtures. 3-D finite element method is adopted and 18-node solid element is selected for more accurate modeling of material properties and temperature field in the thickness direction. For stress analysis, the tensile and compressive stress ratios of the structure under sinusoidal load are investigated for various volume fraction distributions. For thermo-mechanical buckling analysis, the critical temperature gradient with variation of volume fraction distribution is studied. Finally, the optimal design of FGM plates is investigated for stress reduction and improving thermo-mechanical buckling behavior, simultaneously.

2. Modeling and Formulation

A FGM composite plate, composed of ceramic, FGM, and metal layers, of length a, width b, and thickness h is considered. Material properties are assumed to be varied in the thickness direction only and temperature dependent. The volume fraction of metal V_m is given as follows by applying a simple power law distribution.

† 대한항공 한국항공기술연구원
E-mail : carcass1@snu.ac.kr
Tel : (042) 868-6134, Fax : (042) 868-6128
* 서울대학교 기계항공공학부

$$V_m(z)=[1-(z/h)]^n,\ V_c(z)=1-V_m(z) \quad (1)$$

where volume fraction index n indicates the material variation profile through the thickness direction and is a non-negative real number. All temperature dependent material properties P of the common ceramics and metals are expressed as

$$P(T)=P_0(P_{-1}/T+1+P_1T+P_2T^2+P_3T^3) \quad (2)$$

in which T indicates temperature and P_0, P_{-1}, P_1, P_2 and P_3 are constants in the cubic fit of the material property. According to the linear rule of mixtures, the effective material properties P_{eff}, temperature and position dependent, can be obtained as following

$$P_{eff}(T,z)=P_m(T)V_m(z)+P_c(T)V_c(z) \quad (3)$$

where P_m and P_c represent the material properties of the metal and ceramic, respectively.

A three-dimensional finite element model for thin and thick FGM composite plates is developed and an 18-node solid element is used to analyze more accurately the variation of material properties and temperature field in the thickness direction of the structure. Temperature at each node is obtained by solving the steady-state thermo-mechanical equations. For material nonlinear analysis, Newton-Raphson method is used.

The general steady-state heat conduction equation can be expressed as

$$\nabla\cdot(k\nabla T)=0 \quad (4)$$

where k indicates the thermal conductivity and is a temperature and position dependent property, functions of T and z. By applying the Green's theorem and finite element discretization, the following equation is obtained.

$$\sum_e \mathbf{K}_{Te}(\mathbf{T}_e)\mathbf{T}_e=\sum_e \mathbf{R}_{Te} \quad (5)$$

where

$$\mathbf{K}_{Te}(\mathbf{T}_e)=\int(\mathbf{N}_{,x}{}^T k_x\mathbf{N}_{,x}+\mathbf{N}_{,y}{}^T k_y\mathbf{N}_{,y}+\mathbf{N}_{,z}{}^T k_z\mathbf{N}_{,z})dV_e \quad (6)$$

Additionally, $\mathbf{R}_{Te}$ denotes the external thermo-mechanical load. After assembling over all elements, Eq. (6) becomes

$$\mathbf{K_T(T)T=R} \quad (7)$$

This nonlinear equation can be solved for $\mathbf{T}$ using Newton-Raphson method.

Considering a three-dimensional solid body in equilibrium as,

$$\int\delta\mathbf{E}^T\mathbf{S}dV-\delta\mathrm{W}=0 \quad (8)$$

where $\delta\mathbf{E}$, $\mathbf{S}$, $\delta\mathrm{W}$ and V indicate the virtual strain vector expressed in terms of the displacement vector $\mathbf{u}$, the 2nd Piola-Kirchhoff stress vector, the external virtual work and the volume of the undeformed configuration, respectively. The stress vector $\mathbf{S}$ is related to the strain vector $\mathbf{E}$ through the following equations.

$$\mathbf{S=C(E-E^{th})} \quad (9)$$

where $\mathbf{C}$ and $\mathbf{E^{th}}$ is the 6×6 elastic matrix of material stiffnesses and the initial strain vector in thermal environment, respectively. The strain vector $\mathbf{E}$ and the virtual strain vector $\delta\mathbf{E}$ can be written as

$$\mathbf{E}=\mathbf{Bq}_e,\ \delta\mathbf{E}=\mathbf{B}\delta\mathbf{q}_e \quad (10)$$

where $\mathbf{B}$ is a matrix of derivatives of the shape functions. The external virtual work $\delta\mathrm{W}$ is related to the element nodal load vector $\mathbf{Q}_e$ as following.

$$\delta\mathrm{W}=\delta\mathbf{q}_e{}^T\mathbf{Q}_e \quad (11)$$

By substituting Eqs. (9-11) into Eq. (8) and by assembling over all elements, the following equation can be obtained.

$$\mathbf{Kq-Q=0} \quad (12)$$

where $\mathbf{K}$, $\mathbf{q}$ and $\mathbf{Q}$ denote the global stiffness matrix, the global nodal displacement vector, and the global nodal load vector, respectively. Eq. (12) can be solved for $\mathbf{q}$. The stress vector can be obtained by substituting $\mathbf{q}$ into Eqs. (9) and (10).

In order to analyze the thermal buckling behavior, the following eigenvalue problem is considered.

$$\left[\mathbf{K}+\lambda\mathbf{K}^b\right]\mathbf{q}^D=0 \quad (13)$$

where λ, $\mathbf{K^b}$ and $\mathbf{q^D}$ are the eigenvalue, stress stiffness matrix and the associated mode shape, respectively. The critical temperature T_{cr}, corresponds to the lowest eigenvalue of λ, is given by

$$T_{cr}=T_{ref}+\Delta T_{cr}=T_{ref}+\lambda\Delta T \quad (14)$$

Since the matrices $\mathbf{K}$ and $\mathbf{K^b}$ in Eq. (13) are temperature dependent, an iterative scheme is implemented to achieve convergence for critical temperature change ΔT_{cr} ($|\lambda-1|\le 10^{-4}$).

3. Numerical Results

In numerical study, the following dimensionless values are applied.

$$\bar{x}=x/a,\ \bar{y}=y/b,\ \bar{z}=z/h,\ \bar{w}=-w/h$$

$$\bar{\sigma}_x=(\sigma_{xx}/E_m)(a/h)^2 \quad (15)$$

In the stress analysis, the sinusoidal load q distributed over the top surface of the plate is given by the expression

$$q=-\bar{q}\,E_m(h/a)^4\sin\pi\bar{x}\sin\pi\bar{y} \quad (16)$$

The tensile strength σ_{Bt} and the compressive strength σ_{Bc} of FGM plates at each point can be calculated according to the linear rule of mixtures. So as to evaluate the mechanical strength, the stress ratio σ^* is introduced by using the tensile stress ratio $\bar{\sigma}_t$ and the compressive stress ratio $\bar{\sigma}_c$, as following.

$$\sigma^* = \begin{cases} \bar{\sigma}_t = \sigma_{xx} / \sigma_{Bt} & \sigma_{xx} \geq 0 \\ \bar{\sigma}_c = \sigma_{xx} / \sigma_{Bc} & \sigma_{xx} \leq 0 \end{cases} \quad (17)$$

In this equation, to avoid failure, the condition $|\sigma^*| < 1$ should be fulfilled and when $|\sigma^*|$ becomes small, the structure gets better mechanical strength.

In thermo-mechanical analysis, on the top surface of the plate, a heating temperature $\Delta T = T_1$ is applied, while on the bottom surface and the edges of the plate, a room temperature T_{ref} of 300K is kept. For non-dimensionalization of critical temperature, the dimensionless parameter T^* is introduced in the following form.

$$T^* = T_{cr} / T_{Mm} \quad (18)$$

where T_{Mm} indicates the melting point of metal.

To check the validity of present result, firstly the maximum displacement and stress of a fully clamped isotropic square plate under hydrostatic pressure are analyzed. The hydrostatic pressure q_h applied on the top surface is

$$q_h = -\bar{q}\, E(h/a)^4 \bar{x} \quad (19)$$

The numerical results are compared with analytical solution (5). Table 1 presents the maximum displacement $(\bar{w})_{\max}$ and the maximum stress $(\bar{\sigma}_x)_{\max}$. This shows good agreement between the present work and the previous results.

Table 1. Dimensionless maximum displacement and stress of a fully clamped isotropic square plate under hydrostatic pressure (v=0.3, $\bar{q}$ =5)

Dimensionless quantities	Source	
	Analytical (5)	Present
$(\bar{w})_{\max}(\times 10^{-2})$	3.4398	3.4361
$(\bar{\sigma}_x)_{\max}$	1.0020	0.9418

Secondly, the thermal buckling problem of a fully clamped isotropic square plate under uniform or linear temperature rise in x-direction is studied to verify the present code. The numerical results are compared with those of FEM results (6). The temperature rise under uniform temperature rise is expressed as

$$\Delta T = T_1 \quad (20)$$

where T_1 denotes the temperature change. In addition, the temperature rise under linear temperature rise in x-direction is expressed as

$$\Delta T(\bar{x}) = T_2\, \bar{x} \quad (21)$$

where T_2 is the temperature gradient. The critical temperature changes are presented in Table 2. It shows that the present results agree well with those of previous works.

Table 2. Critical temperature change of a fully clamped isotropic square plate under temperature rises (a/h=100, v=0.3, $\alpha = 2\times10^{-6}$)

Temperature distribution	Source	
	FEM (6)	Present
Uniform	167.70	167.65
Linearly varying	332.50	328.92

The optimal design of clamped square ZrO_2/Ti-6Al-4V FGM plates considering stress and critical temperature is investigated. The objective is to obtain the optimal value of volume fraction index n. In this case, the optimization problem is expressed as follows.

Find n

Minimize $f(n) = |\sigma^*|_{\max} - \omega_T T^*$

Subject to $0 \leq |\sigma^*|_{\max} < 1,\ 0 \leq T^*, -n \leq 0$ (22)

By solving Eq. (22), the optimal values of volume fraction index when ω_T is 1.85 and 2.0 are obtained with an accuracy of 0.01 and those are

n=0.12 when ω_T =1.85, n=2.63 when ω_T =2.0 (23)

When the weighting factor is increased, the weighting of thermo-mechanical buckling temperature increases, thus, the optimal volume fraction index becomes larger.

Tables 3-4 illustrate the optimal values of ZrO_2/Ti-6Al-4V FGM plates comparing to the results of ceramic and metal. It is observed that the objective function f of FGM has the smallest value, while that of ceramic has the largest value. In Table 3, $|\sigma^*|_{\max}$ and T^* of FGM are between those of ceramic and metal. However, in Table 4, $|\sigma^*|_{\max}$ and T^* of FGM have the largest values. From the results, by the optimization procedure the FGM can get better stress reduction and thermo-mechanical buckling behavior than both pure ceramic and metal.

Table 3. Optimal values of ZrO_2/Ti-6Al-4V FGM plates (a/h=50, $\bar{q}$ =5, ω_T =1.85, n=0.12)

	$\lvert\sigma^*\rvert_{\max}(\times10^{-3})$	$T^*(\times10^{-3})$	$f(\times10^{-3})$
Ceramic	246.4770	360.6412	-420.7093
Metal	35.92579	294.2868	-508.5047
FGM	53.76075	305.1973	-510.8543

Through-the-thickness distributions of the stress ratio σ^* in cases of n=0.12 and 2.63 are shown in Fig.1. The stress distribution when n is 0.12 shows more smooth response than that when n is 2.63. The tensile stress ratio

of n=0.12 is smaller than that of n=2.63, but the compressive stress ratio of n=0.12 is larger than that of n=2.63.

Table 4. Optimal values of (a)-type ZrO_2/Ti-6Al-4V FGM plates (a/h=50, $\overline{q}$=5, ω_T=2.0, n=2.63)

	$\|\sigma^*\|_{max}$ ($\times 10^{-3}$)	T^* ($\times 10^{-3}$)	f($\times 10^{-3}$)
Ceramic	246.4770	360.6412	-474.8055
Metal	35.92579	294.2868	-552.6477
FGM	252.2609	405.8518	-559.4426

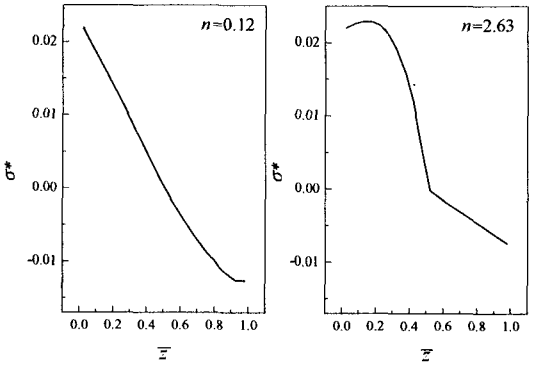

(a) (b)

Fig. 1. Through-the-thickness distribution of the stress ratio σ^* for ZrO_2/Ti-6Al-4V FGM plates (a/h=50, $\overline{q}$=5)

Figs. 2-3 depict the stress ratio σ^* distributions on the top and bottom surfaces of the plates. The difference of tensile and compressive stress ratios in Fig. 2(a) is smaller than that in Figure 3(a). On the contrary, the difference in Fig. 2(b) is larger than that in Figure 3(b). However, the difference on the bottom surface is much smaller than that on the top surface.

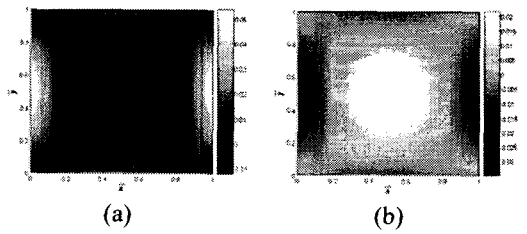

(a) (b)

Fig. 2. Stress ratio σ^* distribution of a ZrO_2/Ti-6Al-4V FGM plate: (a) top surface; (b) bottom surface (a/h=50, $\overline{q}$=5, n=0.12)

As a result, the smaller stress ratio than ceramic and the better thermo-mechanical buckling behavior than metal can be achieved by using FGM plates. In addition, it is shown that the FGM plate can have even better thermo-mechanical buckling behavior than pure ceramic.

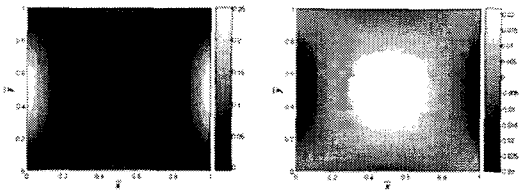

(a) (b)

Fig. 3. Stress ratio σ^* distribution of a ZrO_2/Ti-6Al-4V FGM plate: (a) top surface; (b) bottom surface (a/h=50, $\overline{q}$=5, n=2.63)

4. Conclusions

The optimal design of FGM plates is investigated using 3-D finite element method. Material properties are assumed to be temperature dependent and they are varied continuously in the thickness direction. To obtain the volume fraction, simple power law distribution is applied. The effective material properties, temperature and position dependent, is obtained using linear rule of mixtures. From the results, by using FGM plate, the smaller stress ratio than ceramic and the higher critical temperature than metal can be obtained.

Acknowledgement

This work was supported by the Brain Korea 21 project.

References

(1) Holt, J. B. et al., 1993, Ceramic Transactions: Functionally Graded Materials, Vol. 34, The American Ceramic Society, Westerville.

(2) Na, K. S. Na and Kim, J. H., 2006, Nonlinear Bending Response of Functionally Graded Plates under Thermal Loads, Journal of Thermal Stresses, Vol. 29, pp. 245~261.

(3) Na, K. S. and Kim, J. H., 2005, Three-Dimensional Thermomechanical Buckling of Functionally Graded Materials, AIAA Journal, Vol. 43, No. 7, pp. 1605-1612.

(4) Y. Ootao et al., 2000, Optimization of Material Composition of Functionally Graded Plate for Thermal Stress Relaxation Using a Genetic Algorithm, Journal of Thermal Stresses, Vol. 23, pp. 257-271.

(5) Timoshenko, S. and Woinowsky-Krieger, S., 1959, Theory of Plates and Shells, McGraw-Hill, New York.

(6) Thangaratnam, K. R. et al., 1989, Thermal Buckling of Composite Laminated plates, Computers and Structures, Vol. 32, pp. 1117-1124.